Eksplorium *p*-ISSN 0854-1418
Volume 43 No. 1, May 2022: 29–40 *e*-ISSN 2503-426X

Tectonic Pattern Imaging of Southern Sumatra Region Using Double Difference Seismic Tomography

Akmal Firmansyah[1], Wandono[2], Mohamad Ramdhan[3]*
[1]Center for Earthquake and Tsunami
Indonesian Agency for Meteorology, Climatology, and Geophysics (BMKG),
Angkasa I St., No. 2, Kemayoran, Jakarta 10720, Indonesia
[2]Study Program of Geophysics; School of Meteorology, Climatology, and Geophysics of Indonesia (STMKG),
Pondok Betung, Pondok Aren, Tangerang Selatan, Banten 15221, Indonesia
[3]Research Center for Geological Disaster, National Research and Innovation Agency (BRIN),
Sangkuriang St., BRIN Science and Technology Area, Bandung, 40135, Indonesia
*E-mail: mohamad.ramdhan@brin.go.id

Article received: 15 March 2022, revised: 12 Mei 2022, accepted: 31 Mei 2022
DOI: 10.17146/eksplorium.2022.43.1.6603

ABSTRACT

Southern Sumatra and its surroundings are close to the contact zone of the Indo-Australian plate and Eurasian plate, so the area always relates to the high seismicity zone. The Sumatran subduction zone, the Mentawai fault, and several segments of the Sumatran fault drive seismic activities in the area. Tectonic settings are essential to understanding the area's source and hazard. This understanding can be obtained using the relocated hypocenter distribution and the 3D velocity model in the area. Relocated hypocenters and velocity models are obtained from simultaneous inversion from the BMKG earthquake catalog in January 2012-December 2020 using the double difference seismic tomography method. Seismic velocity inversion of P- and S- wave tomograms image the thermal zone beneath Dempo and Patah volcanoes at a depth of 30-50 km. Slab dehydration is also observed in several forearc high zone. Both phenomena are associated with negative anomalies. The Sumatran and Mentawai fault zones are marked between negative and positive anomalies on the contact zone. The subducted slab of the Indo-Australian plate is observed until a depth of 150 km, which is the maximum depth of nodes used in this study. The granitic basement beneath Anak Krakatau volcano is detected until 10 km. Two of those geological features are related to positive anomalies.

Keywords: seismic tomography, double difference, Southern Sumatra

BACKGROUND

Southern Sumatra and its surroundings are regions with high seismicity. The position bordering the Eurasian continental plate with the Indo-Australian oceanic plate forms a plate subduction system (deformation front) on the west side of Sumatra island. Other sources are various segments of the Sumatran fault (SF) and Mentawai fault zone (MFZ) [1]. Subduction transitions between the southern part of Java island and the western part of Sumatra island formed a graben in Sunda strait [2]. These tectonic features have caused 6,990 earthquakes in the last eight years (BMKG catalog) (Figure 1). Advanced earthquake catalog data processing can be used to understand tectonic conditions in the research area because it produces more precise earthquake parameters.

Earthquake hypocenter relocation is one method to improve earthquake parameter accuracy because the uncertainty value of hypocenter parameters can be minimized with this process. A tectonic study with the seismic tomography method was conducted to describe subsurface structures whose images

can be used to determine earthquake and tsunami-prone areas based on the anomalies information in the image [3]. The tomogram contains seismic velocity perturbation information or relative change between the inverted seismic velocity and the initial model with a positive or negative value. The arrival time of P- and S- waves from each earthquake event was used to calculate the simultaneous inversion between the hypocenter parameters and the velocity model.

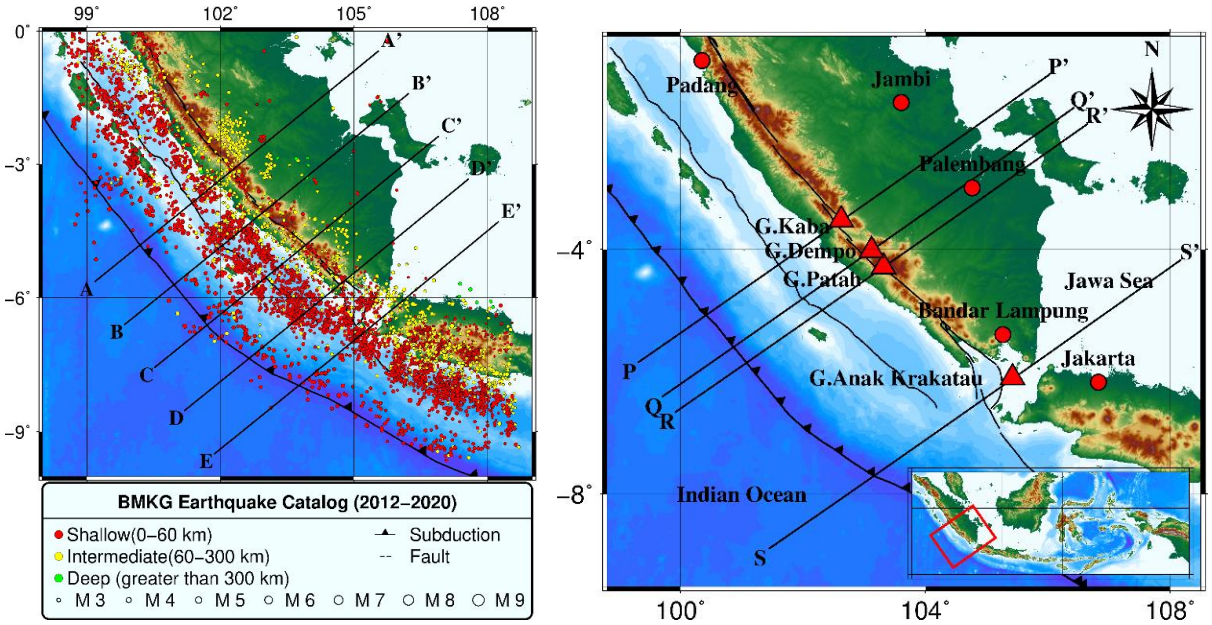

Figure 1. (a) Seismicity map of Southern Sumatra for 2012-2020 from the relocated hypocenter data. A–A' to E–E' lines are the vertical cross-section line shown in Figures 4, 8, and 9, and (b) P–P' to S–S' lines are the vertical cross-section beneath Mount Kaba, Mount Dempo, Mount Patah, and Mount Anak Krakatau shown by Figure 7

Those steps were conducted to obtain the tectonic pattern information in Southern Sumatra and its surroundings which are very useful in understanding the tectonic characters in the research area. This knowledge is instrumental in supporting earthquake disaster mitigation, including regional development planning. The ability will reduce the number of life and infrastructure losses due to earthquakes.

DATA AND METHODS

This study uses P- and S- waves arrival times from 6,990 earthquakes recorded by 130 seismic sensors from Center for Earthquake and Tsunami (PGT), BMKG repository. The data period is January 2012–December 2020 in the area of 96° – 110°E dan 2°N–11°S. Meanwhile, the interpretation is carried out within these four edge points 98.101°E, 4.515°S; 105.131°E, 0.407°N; 108.873°E, 4.937°S; dan 101.843°E, 9.860°S. This data is converted into input format for *tomoDD* using a Python-based program.

Before running the application, it is necessary to do model parameterization. The first model parameter is the initial velocity model as the input model for the tomographic inversion. This study implemented the AK135 model [4]. We determined grid size parameterization to invert the velocity model in the next step. We used 15 nodes on the x-axis, 11 on the y-axis, and 15 on the z-axis with the reference point of 103.544°E dan

p-ISSN 0854-1418
e-ISSN 2503-426X

4.729°S and axes rotation of -35º. The distance used in the x- and y- axes is 65 km between each node. Vp/Vs values are also required in the inversion process. In this study, the value 1.7656 was used based on the Wadati diagram (see Figure 2c).

Tomographic inversion using the double difference method was conducted using the *tomoDD* application [5]. The steps started by pre-processing the data using *ph2dt* to form earthquake pairs and connect them to surrounding earthquakes. The output of *ph2dt* will be used as input to *tomoDD*. Earthquake relocation and tomographic inversion on *tomoDD* were performed using the pseudo-bending ray-tracing method [6]. The appropriate input parameters and damping values determine accurate results.

The results of the inversion process that will be analyzed and interpreted are the relocated hypocenters and the new velocity model anomalies. The analysis also considers the conditional number of damping (CND) value, the trade-off curve, the residual times, and RMS graph of the relocated hypocenter. These parameters are essential parameters to assess whether the inversion is on track. CND value is best within 40–80 [7]. The damping parameter can be changed to obtain a better CND value.

The resolution test used in this study was the Derivative Weighted Sum (DWS) method [8]. This test must be carried out to determine which areas are in good resolution. The DWS method calculates the ray path density at a node. A high DWS value represents a good resolution at a node, and a low DWS value represents the opposite. The area that can be interpreted correlates with DWS value greater than 500 [9].

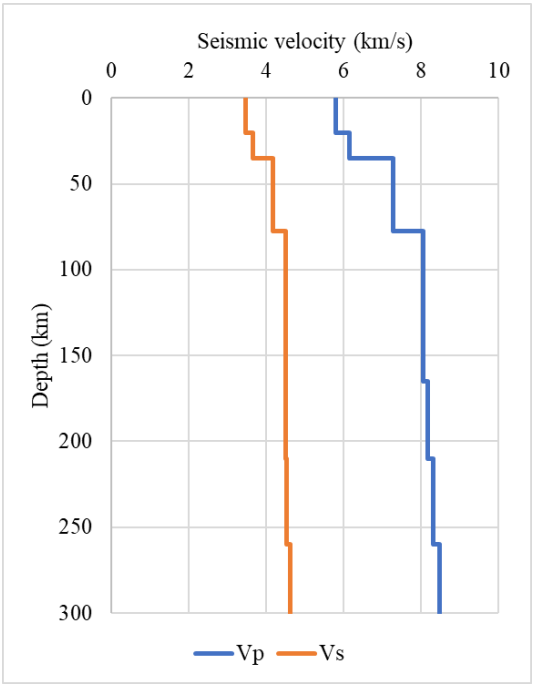

(a)

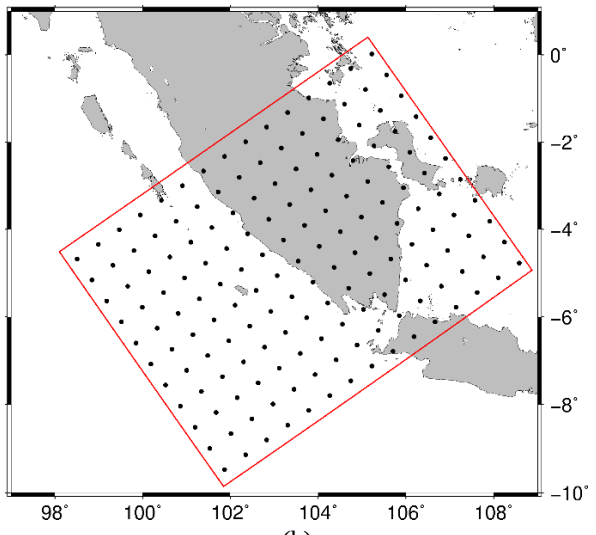

(b)

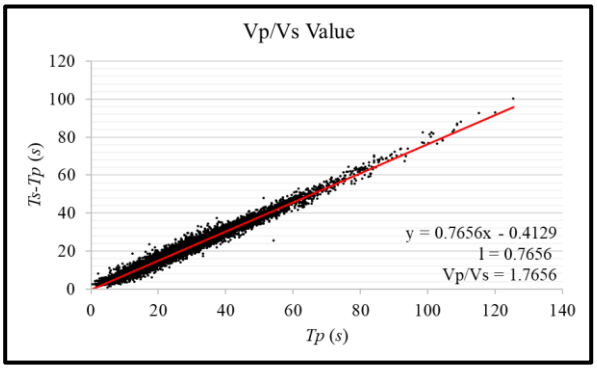

(c)

Figure 2. (a) AK135 velocity model [4] as the initial velocity model. (b) the nodes used in this study, and (c) Wadati Diagram for determining the Vp/Vs value of 1.7656

RESULT AND DISCUSSION

This study succeeded in relocating 6,731 (96.2%) of 6,990 earthquakes. The travel time residual and the RMS value (Figure 3a) are centered around 0 (zero). The majority of earthquakes experience a change in depth from a fixed depth to a more scattered depth. Tectonically, it is more realistic because the depths of the earthquakes are spread over all fault planes. Before the relocation, most earthquakes had a depth of 0–30 km, and after the relocation changed to a depth of 11–70 km (Table 1). Vertical cross-sections were carried out on A–A' to E–E' line (Figure 1a) to illustrate the hypocenter distribution in the vertical dimension.

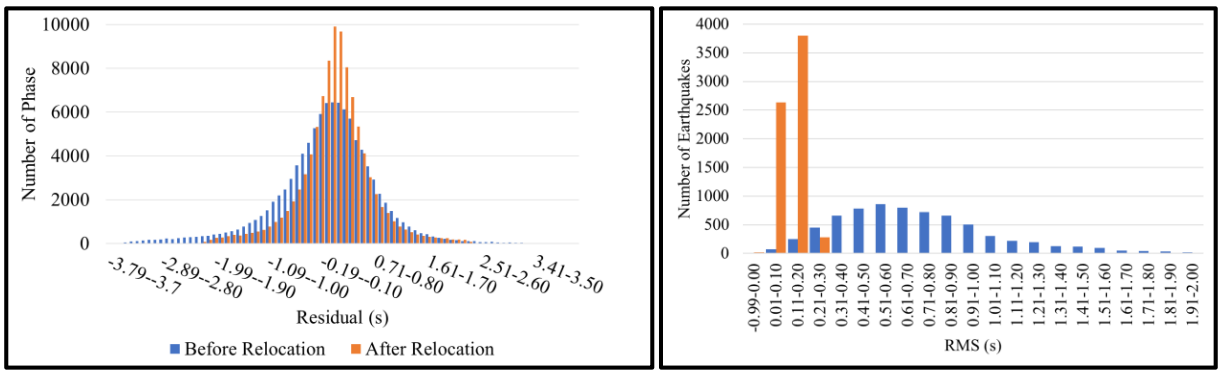

(a) (b)

Figure 3. Comparison of residual (a) and RMS (b) values between before (blue) and after (orange) relocation

Table 1. Comparison of the number of earthquakes before and after the relocation process based on depth

Depth (km)	Before relocation	After relocation
0-10	2.305	96
11-30	2.459	2.002
31-70	1.397	3.252
71-100	309	689
>100	520	692
Total	6.990	6.731 (96,2%)

The relocation cross-section results (Figure 4) show that the hypocenters form a pattern of tectonic structure of the Indo-Australian slab under the Eurasian plate. In addition, the hypocenter is still detected at a depth of 200–300 km. Earthquakes at this depth originated from the Wadati-Benioff zone of the Indo-Australian subducted slab, which has a gentle slope. Moreover, on B, C, and D lines, there are clusters of earthquakes at a depth of <100 km at 300–400 km. They are expected to have originated from the megathrust zone and the Mentawai thrust fault.

The earthquake cluster at a distance of 400–500 km, having a depth of fewer than 50 km, probably originated from the Ketaun, the Manna, and the Semangko segments of the Sumatran fault [2]. In addition, the relocation results also show several zones with earthquake absence marked with red circles. These zones are located in the Mentawai basin, crossed by the Mentawai thrust fault and the forearc high zone. These minimum seismicity zones should be aware of their potential earthquake and tsunami in the future, given their location in the shallow ocean (<60 km).

p-ISSN 0854-1418
e-ISSN 2503-426X

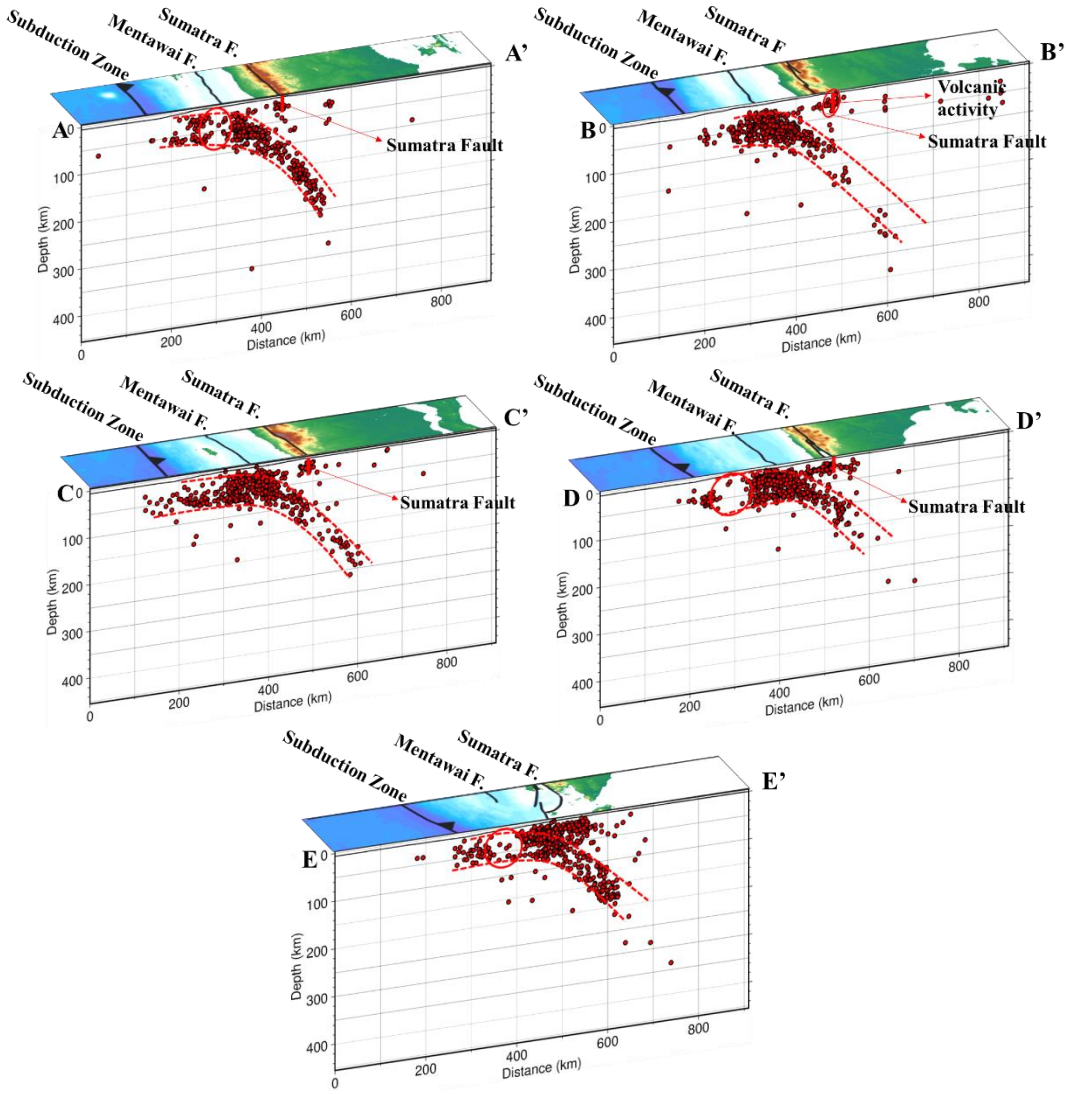

Figure 4. Vertical cross-section from A-A' to E-E' in the study area. The maximum distance of the earthquake hypocenter to each cross-section line is ±250 km. Red dotted lines represent the subducted oceanic slab in the area

The Vp tomogram and its DWS value can be seen in Figure 5. The Vs tomogram and its DWS value can be seen in Figure 6. Both were in good resolution to a depth of 150 km, which is the maximum node in this study.

Positive anomalies can be found alternately with negative anomalies at a depth of 0–20 km. Meanwhile, only positive anomalies exist at a 40–150 km depth. Geological structures in that area cause a positive anomaly with higher Vp and Vs relative to the initial velocity model.

Vertical cross-sections were carried out on both tomograms on A–A' to E–E' lines. There is a positive anomaly on A–A' to D–D' line (Figures 8 and 9), which is associated with the existence of the Indo-Australian plate subduction under the Eurasian plate. The oceanic Indo-Australian plate has a high density which causes a high Vp and Vs value related to a positive anomaly.

The red dotted lines in Figures 8 and 9 illustrate the representation of the subducting slab. This illustration shows a change in the slab dip at a distance of ±350 km (A–A' line), ±450 km (B–B' to D–D' line), dan ±400 km

(E–E' line). The results are consistent with the Slab 2.0 model [10], which shows a change in slab contour density at a 400–500 km distance, which indicates a change in slab subduction dip. This change is primarily caused by the subducted plate age, where the older plate will have a more significant dip [11].

Another striking Vp and Vs positive anomaly is seen beneath the Anak Krakatau volcano at a depth of 10 km. They are caused by the existence of a granitic basement beneath the Anak Krakatau volcano [12], [13]. The illustration can be seen in Figure 7.

Besides positive anomalies, negative anomalies are also caused by lower Vp and Vs values relative to the initial velocity model. A low rock density zone, a fractured or melted zone, or a magma zone in an active volcano cause this low value. These weak zones are generally associated with fault zones where earthquakes occur or fractures filled with fluid, resulting in decreased Vp and Vs values [3].

On the tomogram, negative anomalies can be observed from a 0-30 km depth bordered by a red dotted line. These anomalies lie beneath the volcanoes in this region, namely Mount Dempo, Mount Patah, and Mount Kaba, so they are related to a thermal zone. This zone can be a magma chamber originating from the partial melting of oceanic crust that migrates to the surface and forms a volcano.

The vertical cross-section is made beneath these three volcanoes to view these thermal zones vertically. The results can be seen in Figure 7. The thermal zone beneath Mount Dempo is detected from 30 to 50 km in depth. In Mount Kaba, it can not be imaged clearly. Meanwhile, Mount Patah can be seen to a depth of ±30 km. The Vp and Vs tomograms show a slight difference in the shape of the thermal zone. It is caused by the S- wave arrival time data being much fewer than the P- wave. Generally, S- wave is noisier than P- wave, so it is harder to pick the S- wave onset [12], [14].

On the Vp and Vs tomogram vertical cross-section (Figure 8 and 9), negative anomalies can also be found in the slab illustration in the D-D' and E-E' lines (Figure 9). This negative anomaly in the slab was associated with the presence of slab dehydration. This event happens due to large amounts of water carried by the subducted slab and oceanic crust, both in the pores and in hydrous minerals, releasing water content due to rising temperatures and pressures [15] [16]. The presence of hydrous minerals and water content causes a decrease in rock density and seismic wave velocity, resulting in negative anomaly values.

In addition, negative anomalies in the vertical cross-section can be seen at a 400-600 km distance and a depth of <50 km in A-A' to C-C' and E-E'. On the A-A' to C-C' line, the anomaly is caused by several segments of the Sumatran fault, and on the E-E' line is driven by Ujung Kulon fault. This weak zone with low seismic wave velocity also decreases the Vp/Vs value. It can be seen in Figure 10, where on the A-A' and B-B' lines crossed by several Sumatran fault segments, the Vp/Vs value becomes low or yellow. It follows Lange et al. (2018) [17].

p-ISSN 0854-1418
e-ISSN 2503-426X

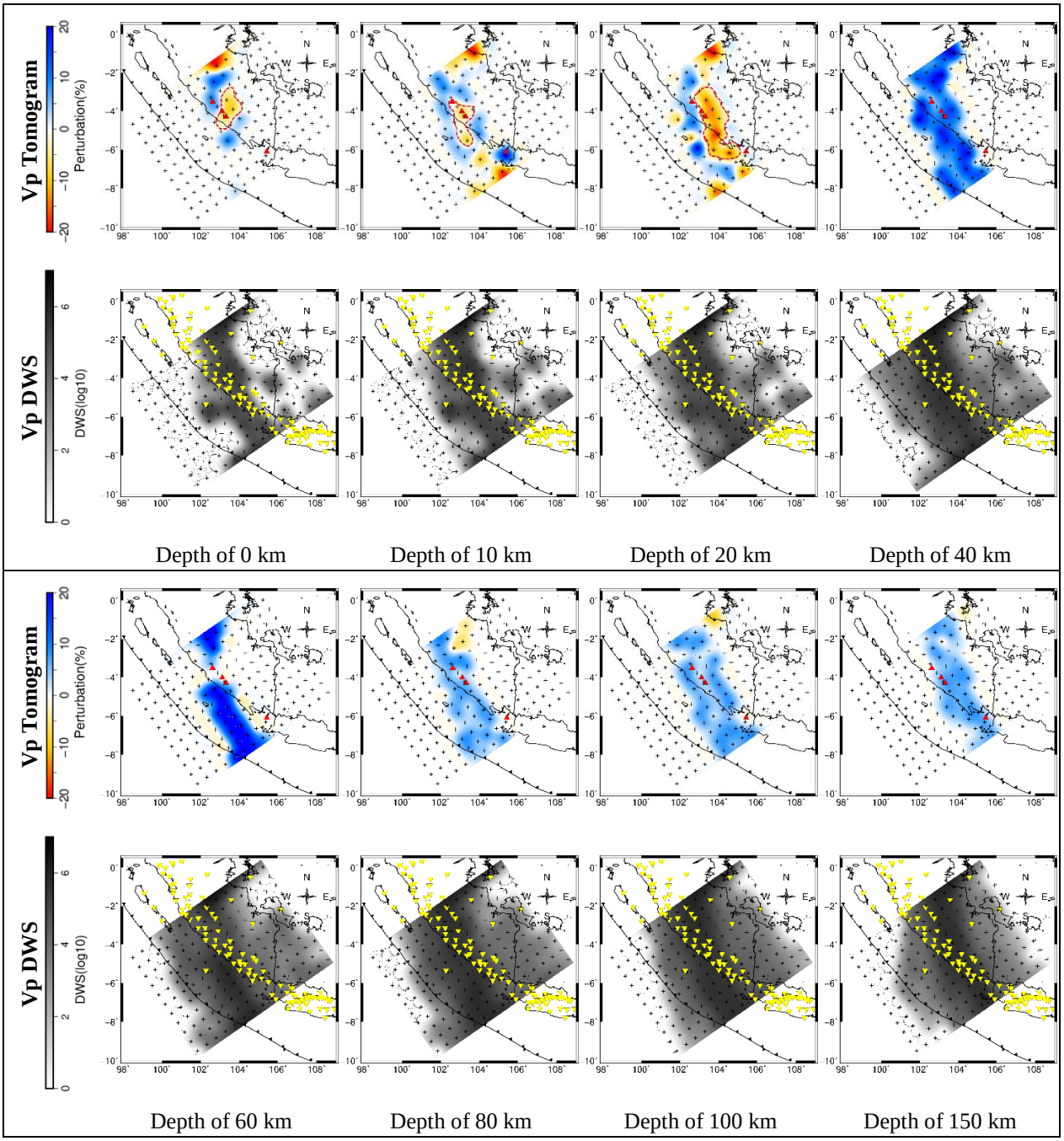

Figure 5. Vp tomogram based on depth from 0-150 km. Yellow reverse triangles represent seismic stations

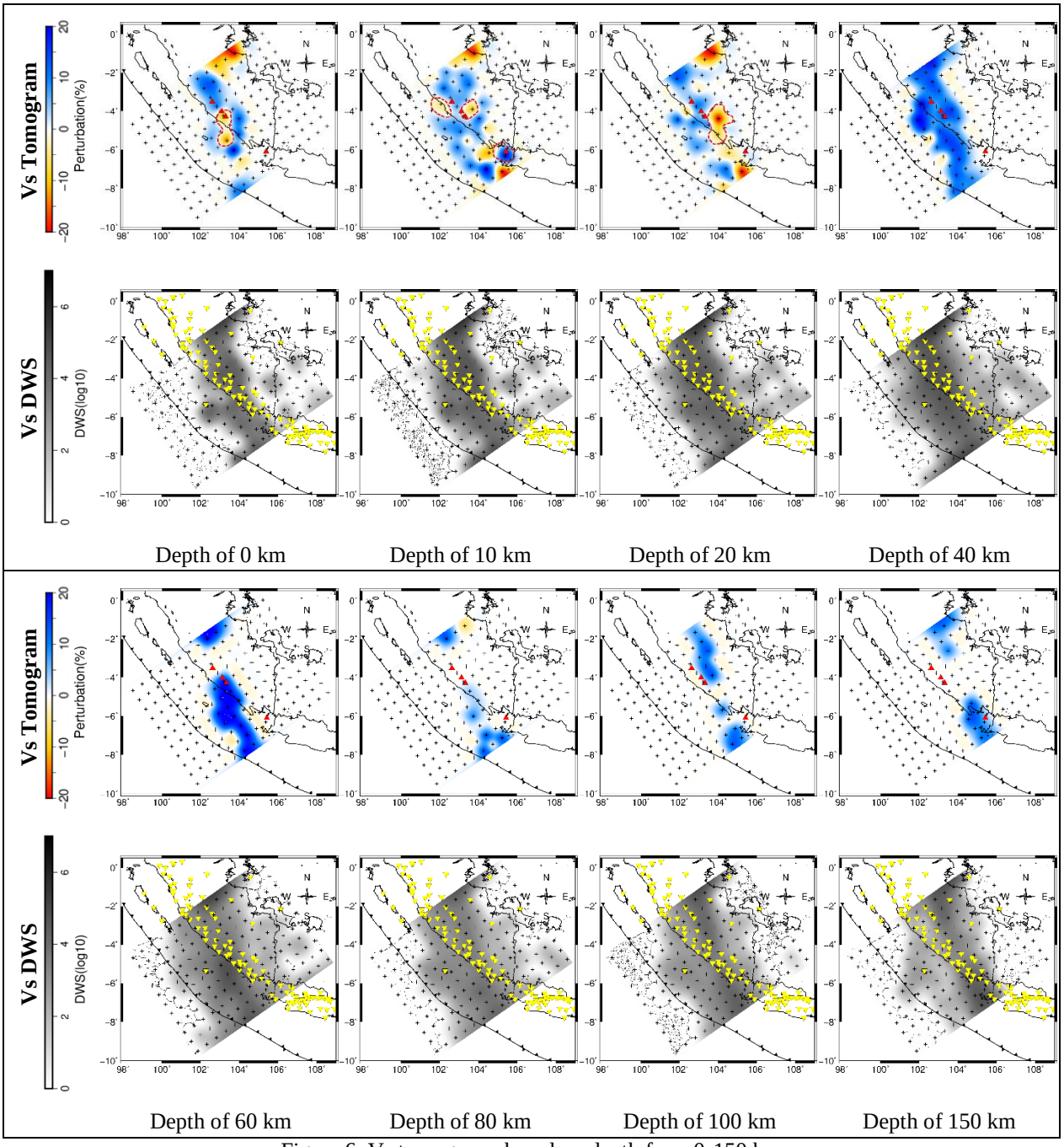

Figure 6. Vs tomograms based on depth from 0-150 km

p-ISSN 0854-1418
e-ISSN 2503-426X

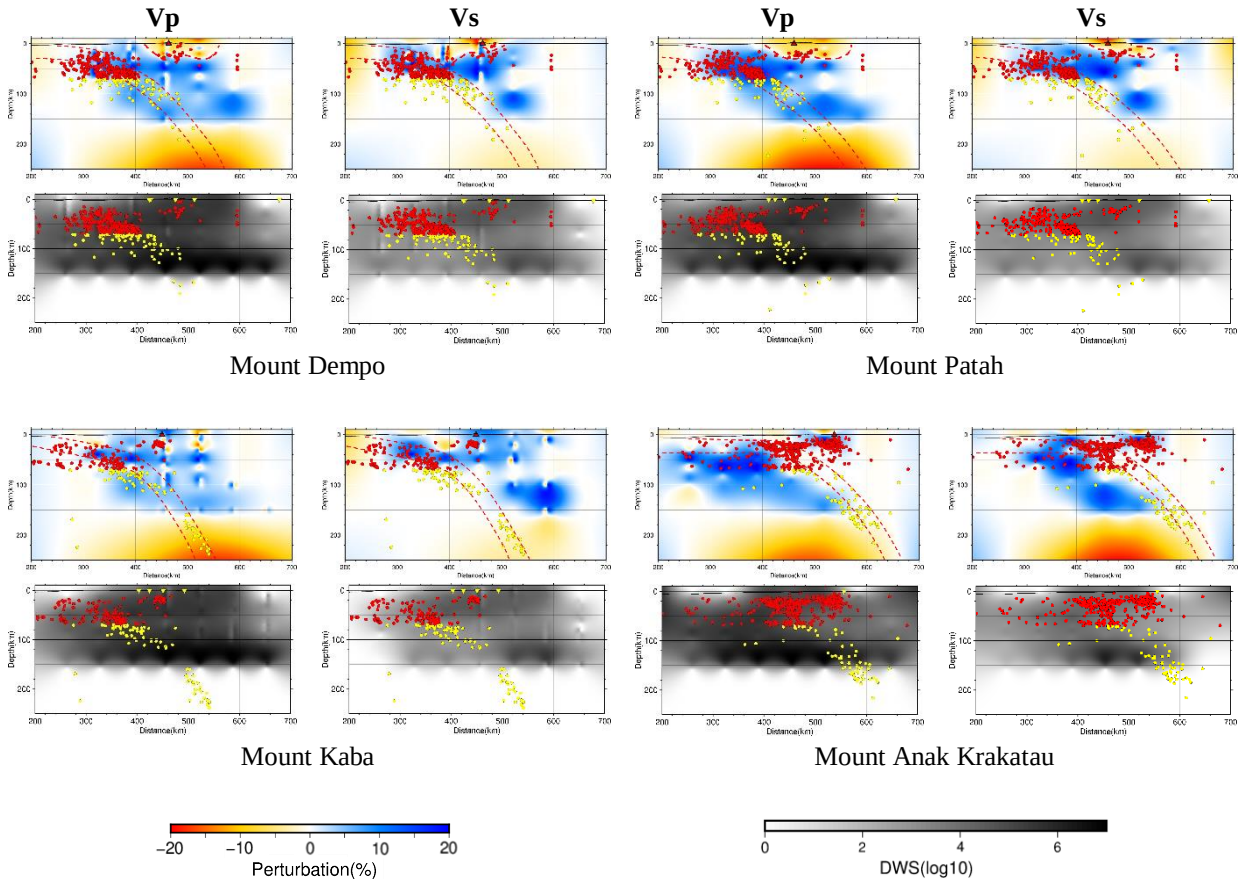

Figure 7. Vertical cross-section for Vp and Vs tomograms with their respective DWS beneath Mount Dempo, Mount Patah, Mount Kaba, and Mount Anak Krakatau. Red dotted lines represent the subducted oceanic slab in the area

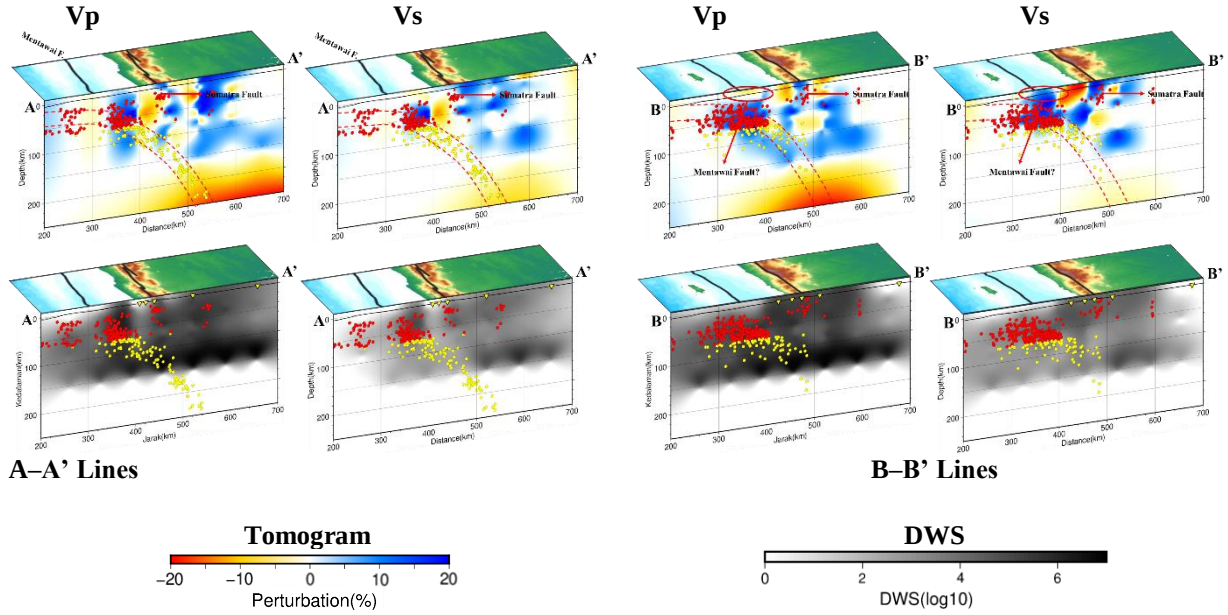

Figure 8. Vertical cross-section of Vp and Vs anomalies with their respective DWS on lines A-A' to B-B'

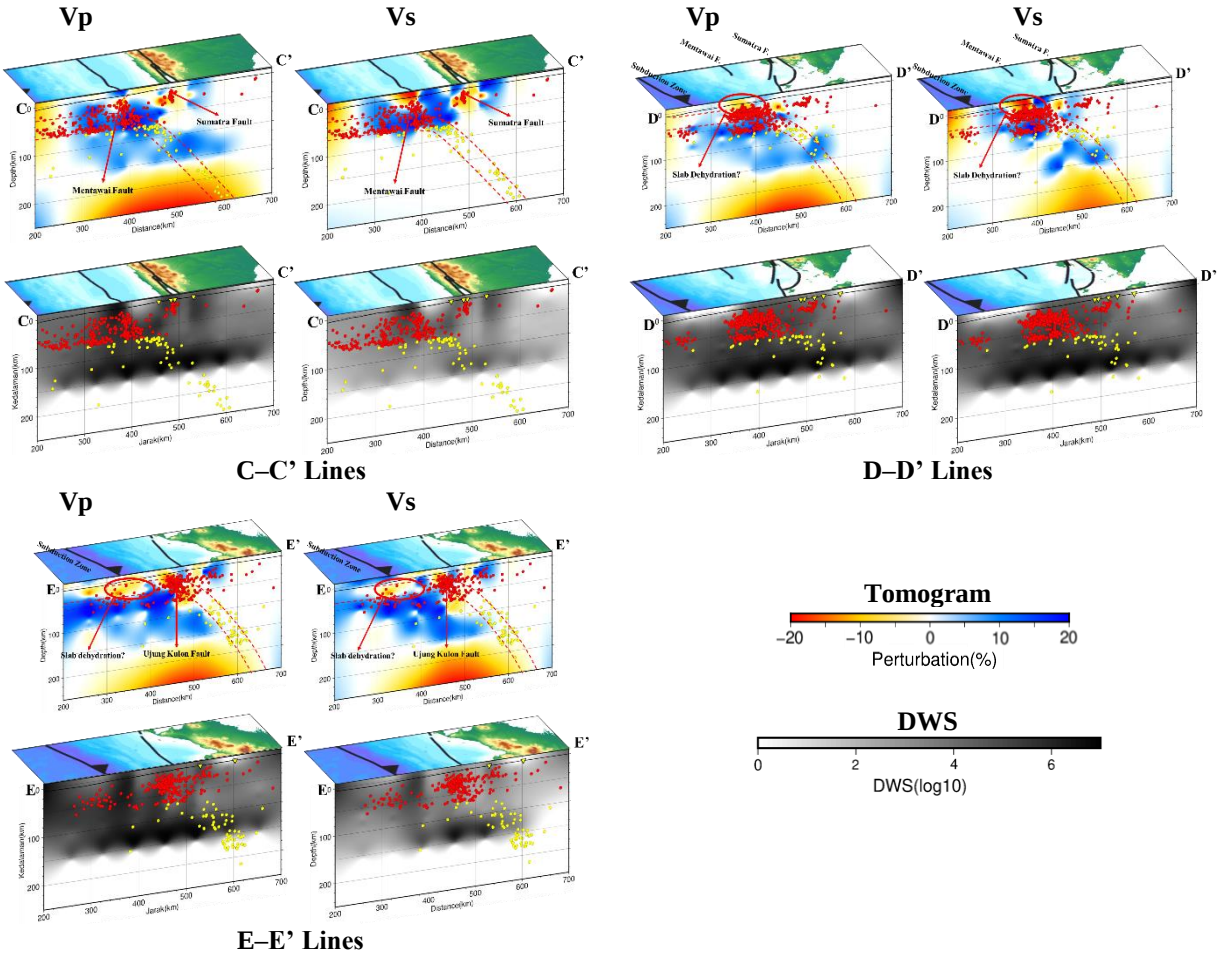

Figure 9. Vertical cross-section of Vp and Vs anomalies with their respective DWS on lines C-C' to E-E'

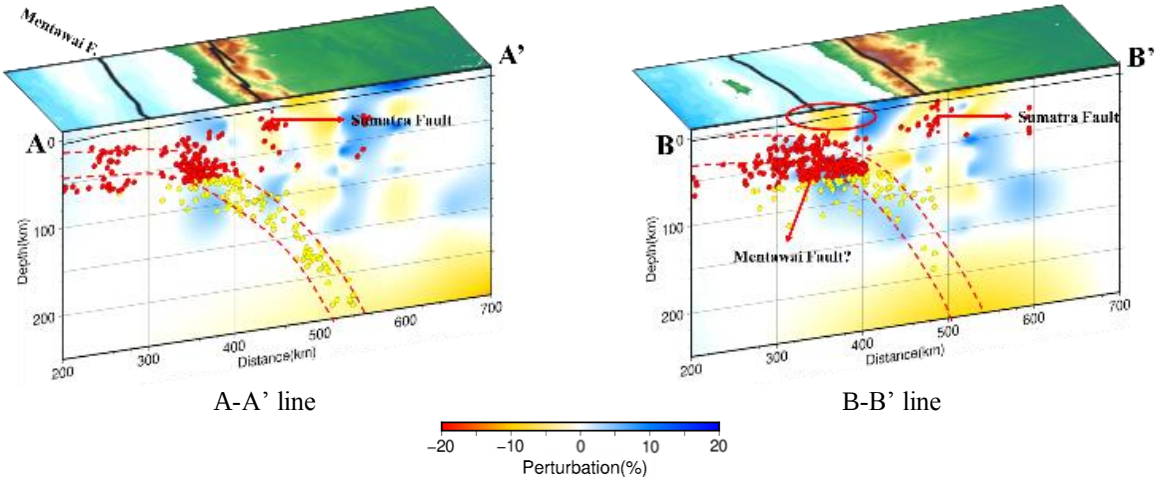

Figure 10. Vertical cross-section of the Vp/Vs values on the A-A' to B-B' line. Red dotted lines represent the subducted oceanic slab in the area. Red dotted lines represent the subducted oceanic slab in the area

CONCLUSION

This study successfully produces a relocated earthquake hypocenter and Vp, Vs, and Vp/Vs tomograms using *tomoDD*. The relocated hypocenter decreased the number of fixed depth earthquakes and changed to the proper depth. This study showed more accurate results based on residual and RMS value evaluation. Earthquake sources identified from the interpretation include the Sumatran subduction zone, the Mentawai fault, and several segments of the Sumatran fault. Vp, Vs, and Vp/Vs tomograms showed good results based on their DWS value. The interpretation results show several tectonic and geological features, namely the Indo-Australian plate slab, several segments of the Sumatran fault, the Mentawai fault, several thermal zones beneath the volcano, and a slab dehydration zone.

ACKNOWLEDGEMENTS

We would like to thank Center for Earthquake and Tsunami (PGT), Indonesian Agency for Meteorology, Climatology, and Geophysics (BMKG) for providing earthquake arrival time data for this research and other parties who contributed to this research. We also thank Mr. Andry Syaly Sembiring for a precious discussion on *tomoDD* software.

REFERENCES

[1] K. Sieh and D. Natawidjaja, "Neotectonics of the Sumatran fault, Indonesia," *J. Geophys. Res. Solid Earth*, vol. 105, no. B12, pp. 28295–28326, 2000, doi: 10.1029/2000jb900120.

[2] PuSGeN, *Peta Sumber dan Bahaya Gempa Indonesia Tahun 2017*. Bandung: Pusat Penelitian dan Pengembangan Perumahan dan Permukiman Badan Penelitian dan Pengembangan Kementerian Pekerjaan Umum dan Perumahan Rakyat, 2017.

[3] R. Maneno and B. J. Santosa, "3d seismic velocity structure imaging beneath Flores region using local earthquake tomography," *J. Phys. Conf. Ser.*, vol. 1245, no. 1, 2019, doi: 10.1088/1742-6596/1245/1/012012.

[4] B. L. N. Kennett, E. R. Engdahl, and R. Buland, "Constraints on seismic velocities in the Earth from traveltimes," *Geophys. J. Int.*, vol. 122, no. 1, pp. 108–124, 1995, doi: 10.1111/j.1365-246X.1995.tb03540.x.

[5] H. Zhang and C. H. Thurber, "Double-difference tomography: The method and its application to the Hayward Fault, California," *Bull. Seismol. Soc. Am.*, vol. 93, no. 5, pp. 1875–1889, 2003, doi: 10.1785/0120020190.

[6] J. Um and C. Thurber, "A Fast Algorithm for Two-Point Seismic Ray Tracing," *Bull. Seismol. Soc. Am.*, vol. 77, no. June, pp. 972–986, 1987.

[7] F. Waldhauser and W. L. Ellsworth, "A Double-difference Earthquake location algorithm: Method and application to the Northern Hayward Fault, California," *Bull. Seismol. Soc. Am.*, vol. 90, no. 6, pp. 1353–1368, 2000, doi: 10.1785/0120000006.

[8] D. R. Toomey and G. R. Foulger, "Tomographic inversion of local earthquake data from the Hengill-Grensdalur Central Volcano Complex, Iceland," *J. Geophys. Res. Solid Earth*, vol. 94, no. B12, pp. 17497–17510, 1989.

[9] H. Zhang and C. Thurber, "Development and applications of double-difference seismic tomography," *Pure Appl. Geophys.*, vol. 163, no. 2–3, pp. 373–403, 2006, doi: 10.1007/s00024-005-0021-y.

[10] G. P. Hayes *dkk.*, "Slab 2, a comprehensive subduction zone geometry model," *Science (80-.).*, vol. 362, no. October, pp. 58–61, 2018.

[11] S. Liu, I. Suardi, X. Xu, S. Yang, and P. Tong, "The Geometry of the Subducted Slab Beneath Sumatra Revealed by Regional and Teleseismic Traveltime Tomography," *J. Geophys. Res. Solid Earth*, vol. 126, pp. 29, 2021, [Daring]. Tersedia pada: https://agupubs.onlinelibrary.wiley.com/doi/epdf/10.1029/2020JB020169.

[12] S. Rosalia, S. Widiyantoro, A. D. Nugraha, and P. Supendi, "Double-difference tomography of P- and S-wave velocity structure beneath the western part of Java, Indonesia," *Earthq. Sci.*, vol. 32, no. 1, pp. 12–25, 2019, doi: 10.29382/eqs-2019-0012-2.

[13] K. Jaxybulatov *dkk.*, "Evidence for high fluid/melt content beneath Krakatau volcano (Indonesia) from local earthquake tomography," *J. Volcanol. Geotherm. Res.*, vol. 206, no. 3–4, pp. 96–105, 2011, doi: 10.1016/j.jvolgeores.2011.06.009.

[14] M. Ramdhan, S. Kristyawan, A. S. Sembiring, D. Daryono, and P. Priyobudi, "Struktur Kecepatan Seismik di Bawah Gunung Merapi dan Sekitarnya Berdasarkan Studi Tomografi Seismik Waktu Tempuh," *Ris. Geol. dan Pertamb.*, vol.

29, no. 2, pp. 227–238, 2019, doi: 10.14203/risetgeotam2019.v29.1047.

[15] R. D. Hyndman and S. M. Peacock, "Serpentinization of the forearc mantle," *Earth Planet. Sci. Lett.*, vol. 212, pp. 417–432, 2003, doi: 10.1016/S0012-821X(03)00263-2.

[16] T. Lestari and A. D. Nugraha, "Imaging of 3-D seismic velocity structure of Southern Sumatra region using double difference tomographic method," *AIP Conf. Proc.*, vol. 1658, no. 2015, 2015, doi: 10.1063/1.4915022.

[17] D. Lange, F. Tilmann, T. Henstock, A. Rietbrock, D. Natawidjaja, and H. Kopp, "Structure of the central Sumatran subduction zone revealed by local earthquake travel-time tomography using an amphibious network," *Solid Earth*, vol. 9, no. 4, pp. 1035–1049, 2018, doi: 10.5194/se-9-1035-2018.